Earthquake Engineering, Tenth World Conference © 1992 Balkema, Rotterdam. ISBN 90 5410 060 5

Arch dams non-linear seismic analysis using a joint finite element

L. Bolognini & P. Masarati
CISE Tecnologie Innovative S.p.A., Milan, Italy
A. Dusi & C. Galimberti
ENEL-DSR-CRIS, Milan, Italy

ABSTRACT: Experimental tests show an influence of construction joints on arch dams dynamic behaviour. The joint behaviour is tipically non-linear and can be taken into account in F.E. analysis using a friction no-tension model: for this purpose a special element was developed and implemented in CANT-SD, a non linear code carried out at CISE for ENEL-CRIS. A summary of the formulation of the joint element is presented, together with a simple test problem chosen among the several ones used for its validation. The paper reports the seismic analysis results of an actual arch dam including joints, compared with the linear ones. Time-history plots of displacements and their Fourier Transforms are presented. The activity performed shows the correct behaviour of the joint element for seismic analyses of arch dams and therefore the code CANT-SD appears to be a useful tool for further investigations necessary for a deeper understanding of joint effects in the actual structural situations.

1 INTRODUCTION

A specific joint finite element was developed to model contact conditions along discontinuity surfaces. This element provides no-tension behaviour as well as friction shear stress: it can be used for static or dynamic three-dimensional structural problems, in the case of small displacements theory.
Such element was implemented in the CANT-SD code (Greco 1987), developed at CISE for ENEL-CRIS with the specific purpose of non-linear seismic analyses: the code tackles material non-linear problems following an implicit time integration method.
The reliability of the solution can be checked, at each step, by means of an energy based control test.

2 JOINT ELEMENT FORMULATION

The essential features of the element may be stated in the following points (Bolognini 1990, Beer 1985):

1. it consists of two isoparametric faces coinciding with those of the three-dimensional elements placed along the discontinuity surface (Figure 1);
2. one local reference system is assumed for each couple of points placed on the two opposite faces;
3. the constitutive model links relative displacements to contact forces, both related to the local system;
4. it has neither mass nor damping.

It is worthwhile to point out that the proposed element allows to model the contact behaviour without introducing any additional variables but nodal displacements already existent.

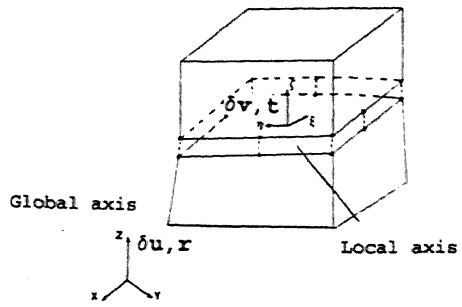

Fig.1 Joint element: geometry, relative displacements field, contact forces

The deformation field is represented by the local relative diplacements vector δv, related to the global nodal displacements vector δu according to:

$$\delta v = B \delta u \qquad B = TN \qquad (1)$$

where T is the transformation matrix and N the shape function matrix.
The stress field is represented by the local surface forces vector t, related to the global nodal forces

vector r according to:

$$r = \int_A B^T t dA \qquad (2)$$

A no-tension constitutive model is assumed between δv and t: if the considered point of the joint turns out to be open, t is set to zero. When the two faces are in contact, the constitutive law is an elastic perfectly plastic one, able to prevent penetration and to reproduce a friction behaviour without dilatancy. The two following relations define the yield surface φ and the plastic potential surface Ψ of such a law:

$$\varphi(t) = \varphi(t_{s1}, t_{s2}, t_n) = \\ = \sqrt{t_{s1}^2 + t_{s2}^2} - t_n tg\alpha \qquad (3)$$

$$\Psi(t) = \Psi(t_{s1}, t_{s2}, t_n) = \sqrt{t_{s1}^2 + t_{s2}^2} \qquad (4)$$

where α is the friction angle.
Following the classic elastoplastic theory, the equations (3) and (4) lead to the incremental elastoplastic stiffness matrix of the material:

$$\dot{t} = D^{ep}\, \delta\dot{v} \qquad (5)$$

The incremental stiffness matrix of the finite element, for contact and plastic flow condition, results therefore:

$$K^{ep} = \int_A B^T D^{ep} B dA \qquad (6)$$

It can be noticed that such a matrix is unsymmetric, as a consequence of the non associated nature of the elastoplastic model. Unsymmetric matrices arise also in the case of some geomechanical material models treated by the code: for this purpose CANT-SD is supplied with a frontal solver for unsymmetric matrices developed for exploiting vector and parallel features of shared memory multiprocessors (Brusa 1990).

3 TEST PROBLEM

The essential features of a simple impact problem (Ayari 1988) are shown in Figure 2, together with CANT-SD results (Bolognini 1990). A time step $\Delta t = T/1500$ was used in proximity of the impact instant and $\Delta t = T/20$ otherwise, being T the period of the mass-spring system. The reported solution is quite coincident with the analytical one and the error in the energy content resulted less than 0.6%

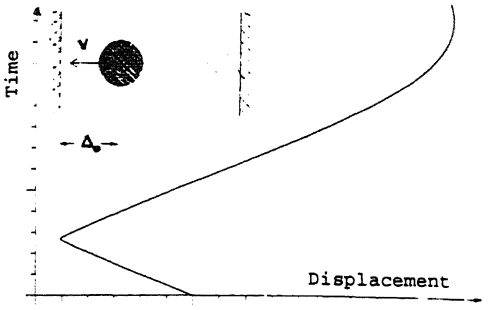

Fig.2 Impact problem: mass-spring model and solution

4 ARCH DAM SEISMIC ANALYSIS

The seismic analysis of the actual Ambiesta (Italy) arch dam (Figure 3) was performed in order to investigate the importance of joint effects in modifying the linear results.

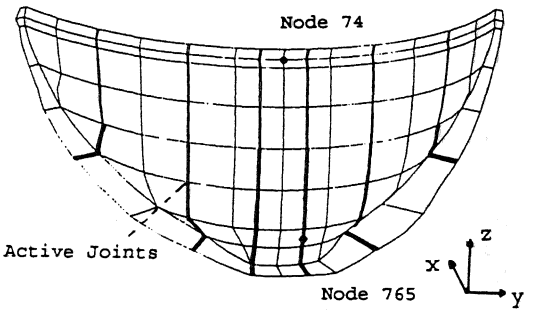

Fig.3 Ambiesta dam: finite element mesh

The construction joints were supposed to be active in the lower part of the dam (Figure 3): such a condition might be due to the coupling of low temperature and empty basin, as indicated by experimental data. The active joints were characterized by initial gap set to zero and friction angle $\alpha = 30°$. The concrete was considered as an elastic material, with a constant damping matrix equivalent to a modal damping factor $\nu = 0.02$ at a frequency of 5Hz.
The structure was subjected to self-weight and to a seismical excitation acting in the three cartesian directions x, y, z, following a nearby site earthquake recorded on 6/7/1976. The maximum ground acceleration was 0.4 g in the horizontal direction and 0.3 g in the vertical one. The time interval analyzed was of about 11 seconds, after which the strong motion effects may be considered negligible.
A constant time step $\Delta t = 0.00488$ sec. was adopted for both linear and non-linear analyses, leading to 2288

steps: the code ran on the multiprocessor Alliant FX80, requiring about 6h cpu-time for the linear analysis and about 40h for the non-linear analysis.
The error in the energy content resulted less than 2% in the former case and less than 4% in the latter. Further possibilities for checking the correct working of the joint element are supplied by the Figures from 4 to 7.

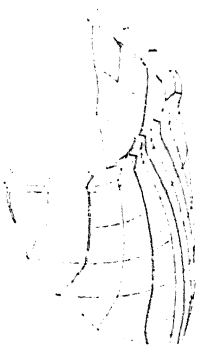

Fig.4 Ambiesta dam: deformed geometry corresponding to maximum displacement of node 74

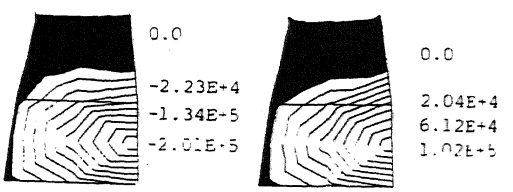

Fig.5 Ambiesta dam: contour lines for normal (left) and tangential (right) stresses along the surface of a construction joint, [Pa]; black area means open joint

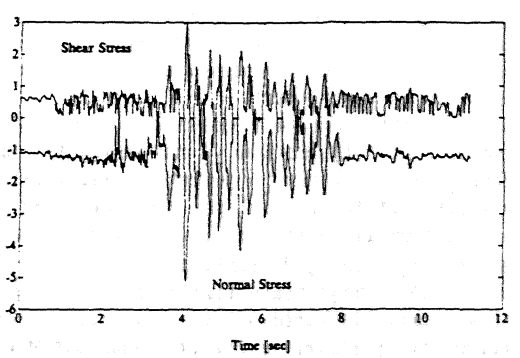

Fig.6 Ambiesta dam: plots of normal stress (below) and tangential stress (above) on the surface of a construction joint, [10^5 Pa]

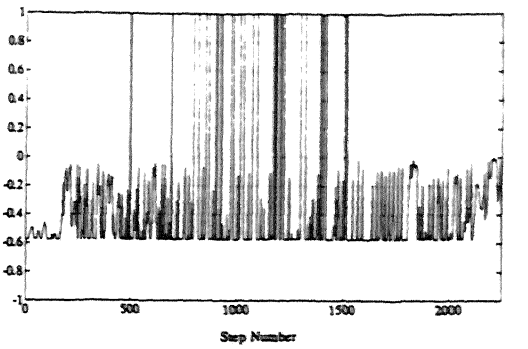

Fig.7 Ambiesta dam: rate between shear stress and normal stress plotted in Figure 6; value 1 means open joint, value -0.578 means plastic sliding.

The Figures from 8 to 13 show the time-history plots for the three displacement components of a point placed at the middle of the crest arch (see node 74 on Figure 3).
The comparison between linear and non-linear time-histories leads to the following considerations.

1. Maximum values for all the components are almost identical during the strong motion period.
2. In the following period wider discrepancies may be observed in x and z components, which are greater in the non linear case (this might be due to the lower global damping related to a reduced overall continuity in the structure).

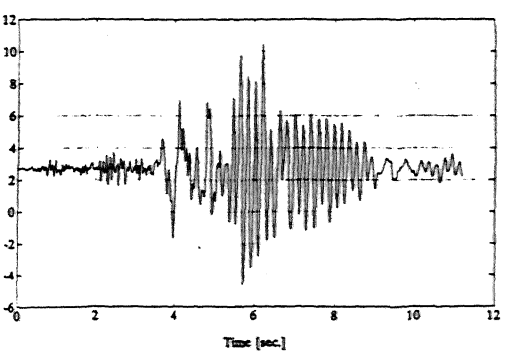

Fig.8 Ambiesta dam: linear analysis, displacement X node 74, [10^{-3} m]

The Figures from 14 to 19 show the Fourier Transform (F.T.) plots for the previous time-histories. The comparison between linear and non-linear Fourier Transforms leads to the following considerations.

1. The maximum peak frequencies may be considered identical (5.22 Hz for x and z components

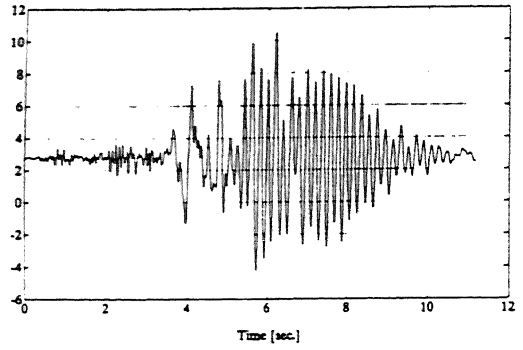

Fig.9 Ambiesta dam: non-linear analysis, displacement X node 74, [10^{-3} m]

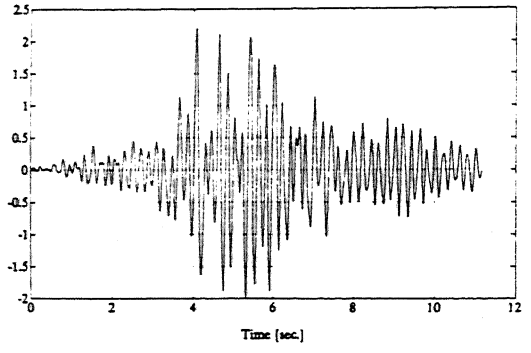

Fig.10 Ambiesta dam:linear analysis, displacement Y node 74, [10^{-3} m]

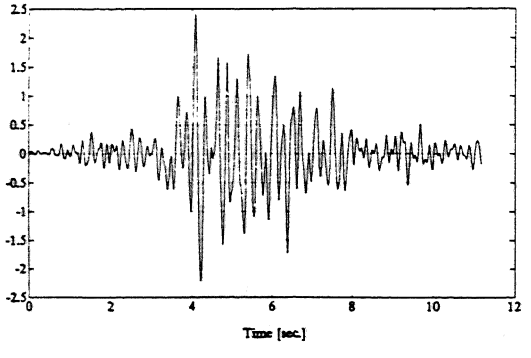

Fig.11 Ambiesta dam: non-linear analysis, displacement Y node 74 [10^{-3} m]

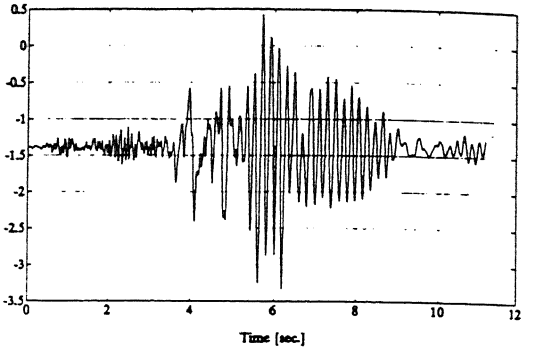

Fig.12 Ambiesta dam:linear analysis, displacement Z node 74, [10^{-3} m]

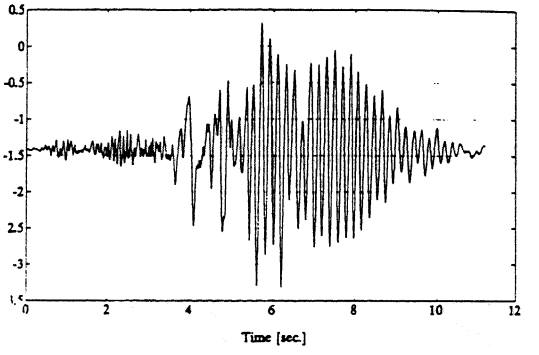

Fig.13 Ambiesta dam: non-linear analysis, displacement Z, node 74 [10^{-3} m]

and 5.0 Hz for y component).

2. The amplitude of the maximum peak increases of about 30% in the non-linear case for x and z components, while it results more than halved for y component.

3. The peaks of frequency lower than 5.0 Hz, owed to the frequency content of the earthquake, are almost identical for x and z components while they result a bit increased for y component.

The different behaviours observed for x and z components, compared with y, may be due to what follows: the two former components are related to the symmetric modal linear shapes while the latter is related to the anti-symmetric ones, and both groups of shapes are excited by the earthquake.

The results of the particular analyzed problem seem to show scarce influence of the presence of the construction joints on the structural behaviour of the crest arch, normally the most stressed part of the dam under seismic loading.

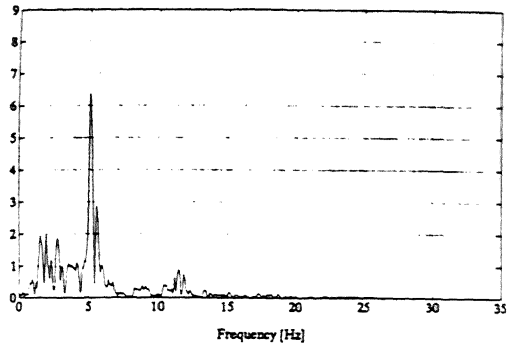

Fig.14 Ambiesta dam: linear analysis, F.T. module of displacement X node 74, [10^{-3} m sec]

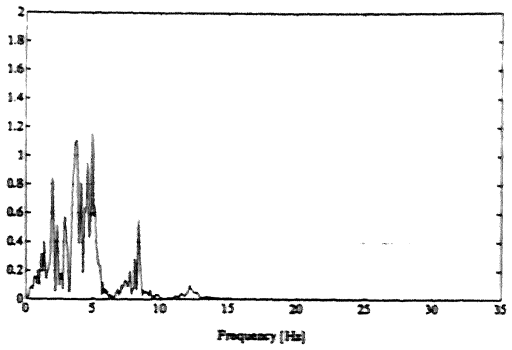

Fig.17 Ambiesta dam: non-linear analysis, F.T. module of displacement Y node 74, [10^{-3} m sec]

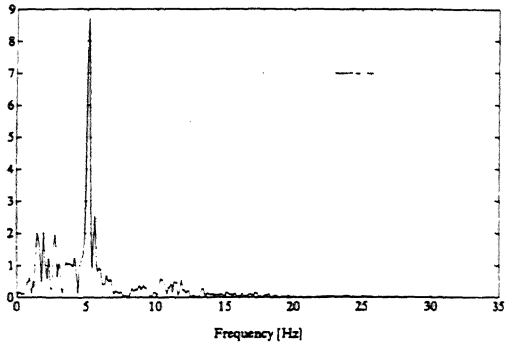

Fig.15 Ambiesta dam: non-linear analysis, F.T. module of displacement X node 74, [10^{-3} m sec]

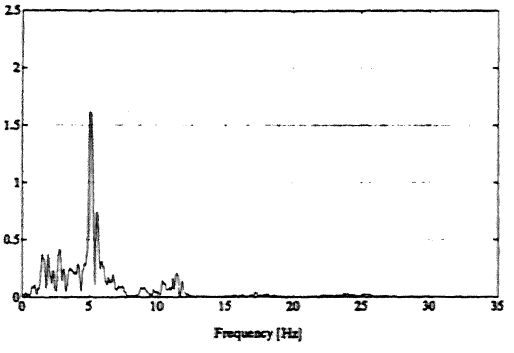

Fig.18 Ambiesta dam: linear analysis, F.T. module of displacement Z node 74, [10^{-3} m sec]

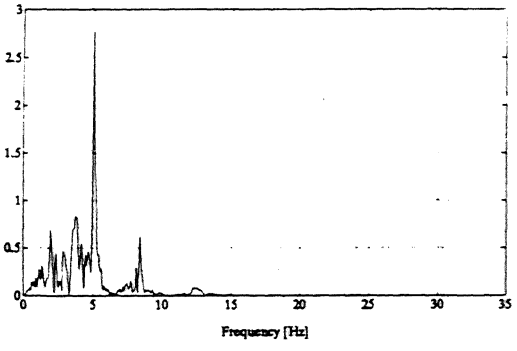

Fig.16 Ambiesta dam: linear analysis, F.T. module of displacement Y node 74, [10^{-3} m sec]

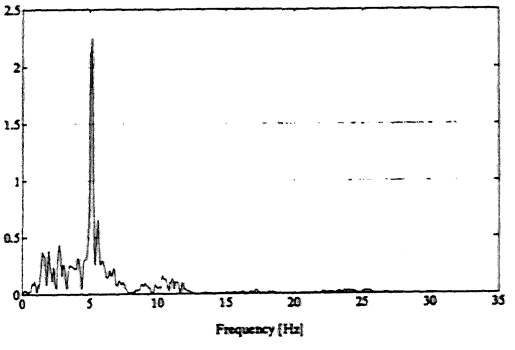

Fig.19 Ambiesta dam: non-linear analysis, F.T. module of displacement Z node 74, [10^{-3} m sec]

5 CONCLUSIONS

The validation of the proposed joint finite element allowed to prove its reliability to solve structural dynamic problems involving contact phenomena.
The specific seismic analysis described in the paper must be considered as a first step towards a systematic use of CANT-SD code to study seismic non-linear response of arch dams.
Such analysis may be regarded as a significative test bench for the numerical model; on the other hand it does not exhaust the matter of constuction joints effects, as several active joints distributions appear to be as realistic as the chosen one.
The non-linear effects induced by the joints, though correctly represented by the model, did not turn out to be very important on the global response of the structure; a deeper influence can be reasonably expected in the following situations:

1. active construction joints spread up to the crest arch;
2. dam without crest arch;
3. initial gap of the joints different from zero.

A preliminary understanding of the importance of the above-mentioned aspects can be drawn by carrying out a group of seismic analyses similar to the presented one, each of them dealing with one single aspect at a time.
An exhaustive study of the problem would require an adequate experimental support in order to provide information about the state of the joints (position, gap, friction angle) for the very dam under analysis.

REFERENCES

Ayari, L. and Saoun, E. 1988. A fracture mechanics based seismic analysis of concrete gravity dams using discrete cracks. Proc. International Conference on Fracture and Damage of Concrete and Rocks, Wien.

Beer, G. 1985. An isoparametric joint/interface element for finite element analysis. International Journal for Numerical Methods in Engineering, Vol. 21.

Bolognini, L. and Masarati, P. 1990. Analisi dei problemi di contatto e formulazione di un elemento finito di giunto da inserire nel codice di calcolo CANT-SD. Rapporto finale CISE 5286.

Bolognini, L. and Masarati, P. 1990. Validazione numerica dell'elemento finito di giunto, nell'ambito del codice di calcolo CANT-SD. Rapporto finale CISE 5851.

Brusa, L. and Riccio, F. 1990. Direct linear equation solver for finite element computations on shared memory multiprocessors. Supercomputing Tools for Science and Engineering, Ed. Franco Angeli.

Greco, A. and Masarati, P. 1987. Il programma CANT-SD per l'analisi elastoplastica statica e dinamica di strutture tridimensionali. Rapporto finale CISE 3494.